*minerals*

MDPI

*Article*

# Experimentation of Heat-Insulating Materials for Surrounding Rocks in Deep Mines and Simulation Study of Temperature Reduction

**Hongwei Deng and Yuanzhe Xiao ***

School of Resources and Safety Engineering, Central South University, Changsha 410083, China
* Correspondence: 225512140@csu.edu.cn

**Abstract:** With the increasing depletion of shallow resources, mining has gradually shifted to deeper levels, and the high-temperature problem of deep mining has restricted the efficient and safe development of mining. In this study, five types of thermal insulation materials for surrounding rocks with different ratios were produced using tailings, P.O.32.5 clinker, aluminum powder, glass beads, quick lime, and slaked lime as test materials. Based on the uniaxial compression test, the thermal constant analysis test, and numerical simulation analysis technology, the change rule of mortar compressive strength and thermal conductivity was analyzed, and the cooling effect of surrounding-rock thermal insulation materials with different ratios was discussed. The results showed that the compressive strength of the surrounding-rock thermal insulation materials ranged from 0.39 to 0.53 MPa, and the thermal conductivity ranged from 0.261 to 0.387 W/(K·m), with the compressive strength of ratio E being the largest and the thermal conductivity of ratio A being the lowest. In the numerical simulation analysis results, the thermal insulation layer thickness was taken as a value of 10 cm when, at this time, the best thermal insulation effect and economic benefits involved a temperature reduction of 0.9 K. In the case of changing the thermal conductivity and inlet wind speed, the original temperature of the rock temperature reduction was also very clear, with maximum reductions of 0.92 K, 0.92 K, and 1.42 K.

**Keywords:** high-temperature mines; thermal insulation material; roadway cooling; numerical simulation



**Citation:** Deng, H.; Xiao, Y. Experimentation of Heat-Insulating Materials for Surrounding Rocks in Deep Mines and Simulation Study of Temperature Reduction. *Minerals* **2024**, *14*, 938. https://doi.org/10.3390/min14090938

Academic Editors: Alexandra Guedes, Shiyu Zhang, Erol Yilmaz and Chen Hou

Received: 10 August 2024
Revised: 5 September 2024
Accepted: 11 September 2024
Published: 13 September 2024



## 1. Introduction

Deep mining has become the primary trend in current mineral resource development. With an increase in mining depth, the problem of thermal damage in deep shafts is becoming increasingly serious [1,2]. The high-temperature underground working environment can lead to mining accidents, affecting miners' work efficiency and physical and mental health and seriously restricting efficient and safe mining [3]. Therefore, it is of great significance to research deep-well thermal damage management technology [4].

At this time, the primary solution to the problem of heat damage in high-temperature mines is ventilation optimization. However, when ventilation optimization fails to achieve the purpose of heat damage control, other auxiliary methods are still needed to control the high-temperature underground environment. Roadway thermal insulation is an active cooling method performed by spraying thermal insulation materials on the surface and inside of the surrounding rock on high-ground-temperature roadways to prevent the heat inside the surrounding rock from spreading into the roadway's wind flow [5]; the surrounding rock is then supplemented with ventilation and other measures to take away the heat in time to realize roadway cooling [6]. The preparation of thermal insulation materials suitable for the underground environment can effectively reduce heat conduction, heat convection, and heat radiation and reduce the cooling costs of underground mining. This is of great significance in preventing thermal damage, creating a suitable working environment, and improving production efficiency [7].

In the mining process, a large number of tailings are produced. At present, there are three main ways to deal with tailings: first, as a pit-filling material, directly using tailings mixed with cement to fill the mine's open area; second, extracting valuable metals from tailings as renewable secondary resources; and, third, as a raw material for preparing thermal insulation material for surrounding rocks according to the characteristics [8,9]. Some scholars, in preparing surrounding-rock thermal insulation material research, have also used tailings as one of the primary raw materials for preparing thermal insulation material. Tailings are ore body particles, and their strength can reduce the amount of clinker and also assist in acting as a skeleton support; in addition, tailings are the ore body's source of materials, so there is no rejection of chemical reactions, and the introduction of new chemical elements leads to elemental pollution and other issues. Tailings also have a certain degree of cementation to ensure good cementation properties [10]. Huiskes, D et al. [11] successfully developed a thermal conductivity insulator with low dry density and low thermal conductivity by incorporating porous expanded glass as a lightweight aggregate in a mineral polymer formed by compositing based on slag. Demirba, R et al. [12] analyzed the effect of two materials, fly ash and silica fume, on expanded perlite lightweight concrete. Their findings showed that adding two mineral admixtures, fly ash and silica fume, to expanded perlite lightweight concrete resulted in a decrease in thermal conductivity of 14% to 18% and a decrease in bulk weight of 8%. Soltan, A et al. [13] utilized granite, kaolinite, and tailings mixed and fired into clay bricks with closed pores and good durability.

From the above, it can be seen that the thermal insulation material prepared using tailings can reduce deep-well thermal damage problems caused by high temperatures in the roadway. Currently, we are accelerating the structural transformation of the green economy and improving the utilization efficiency of solid-waste resources [14]. The scientific promotion of the development of solid-waste resources is a hot research issue that needs to be expanded in the long term. Therefore, it will be of great practical significance if the tailings generated can be effectively recycled and utilized in the process of developing mineral resources [15]. On the one hand, this process can promote the transformation of secondary resource utilization and reduce the accumulation of tailings, pollution, and other problems. On the other hand, it can also reduce the cost of maintaining tailing ponds and improve the economic rationality of their revenue [16]. However, most of the thermal insulation materials prepared face the problem of practical application, and verifying the effect will be a substantial economic problem, so some scholars use numerical simulation to study the effect of the prepared thermal insulation materials. For example, Yao et al. [17] used COMSOL Multiphysics to analyze the coupling of stress and temperature fields to verify the reasonableness of the thermal insulation material they prepared and tested in a field application. Hou et al. [18] used basalt fibers, clinker, and ceramic grains to prepare a thermal insulation material for mines and used COMSOL to verify that the material had a better thermal insulation effect than ordinary concrete.

In this study, five kinds of surrounding-rock thermal insulation materials with different ratios were made with Guangxi Gaofeng Mine's tailings, P.O.32.5 cement, aluminum powder, Vitrified Micro Bubbles, quick lime, and slaked lime as the test materials. Based on the uniaxial compression test, thermal constant analysis test, and numerical analysis technique, the variation rule of mortar compressive strength and thermal conductivity was analyzed, and the cooling effect of thermal insulation materials with different ratios in the surrounding rock was explored. This study will provide valuable insights into future mine heat damage control.

## 2. Experimental Program Design

### *2.1. Raw Material*

Guangxi Gaofeng Mine tailings, P.O.32.5 cement, aluminum powder, glass beads, Vitrified Micro Bubbles (VMB), quick lime, and slaked lime were used to prepare tailings-based thermal insulation material. The Gaofeng mine tailings were selected as the primary material. Large particles of tailings served as aggregates, providing structural support,

while small particles assisted the cement in bonding. These tailings were primarily sourced from the small mine body in the southern part of the −250 m to −200 m level of Gaofeng Mine, known for its high hardness, and were extracted using the upward approach filling mining method. The primary material's particle size distribution and chemical composition are detailed in Tables 1 and 2.

**Table 1.** Tailings' particle size distribution.

| Particle Size/μm | −10 | −20 | −50 | −100 | −200 | −500 | −1000 |
|---|---|---|---|---|---|---|---|
| Separate cumulative/% | 7.73 | 9.01 | 7.49 | 8.12 | 17.01 | 10.87 | 2.79 |
| Total cumulative/% | 20.62 | 29.63 | 46.08 | 64.81 | 81.82 | 97.21 | 100 |

**Table 2.** Chemical composition of tailings.

| Chemical Composition | $SiO_2$ | $Al_2O_3$ | CaO | MgO | Fe | Sn | Sb | Zn | Pb | S | Other |
|---|---|---|---|---|---|---|---|---|---|---|---|
| Content (%) | 41.6 | 2.3 | 18.9 | 0.8 | 5.3 | 0.3 | 0.3 | 1.2 | 0.3 | 5.8 | 23.2 |

P.O.32.5 clinker is selected as the primary cementing material, and the cement grade and dosage are determined by balancing cost and cementing effectiveness. The tailings contain trace heavy metal elements, such as Pb, Zn, Sn, and Sb, which can affect the thermal insulation performance of the material. Ordinary silicate cement, specifically P.O.32.5, is chosen for its superior cementing properties. On the one hand, because the primary raw material tailings have the essential mechanical strength, it is sufficient to select a lower grade of clinker. On the other hand, the lower grade and dosage of clinker can reduce the material cost. Aluminum powder is a chemical foaming agent, which takes the role of foaming slurry, making the material form a dense microporous structure. Quick lime and slaked lime adjust the pH of the slurry to create alkaline conditions suitable for slurry cementation and foaming.

The chemical composition of VMB is shown in Table 3. Its bulk density ranges from 80 to 130 kg/m$^3$, with a thermal conductivity of 0.032 to 0.045 W/(K·m). The glass content exceeds 95%, and the water absorption rate varies between 20% and 50%. VMB exhibits high particle strength, stable physical and chemical properties, excellent aging resistance, and outstanding thermal insulation and fire resistance. When added to the slurry, VMB enhances its flowability and compressive strength while reducing shrinkage. Additionally, incorporating VMB lowers the water absorption rate, improves the material's thermal insulation performance, and enhances its mechanical properties.

**Table 3.** Chemical composition of Vitrified Micro Bubbles.

| Chemical Composition | $SiO_2$ | $Al_2O_3$ | CaO | MgO | $K_2O$ | $Fe_2O_3$ | Other |
|---|---|---|---|---|---|---|---|
| Content (%) | 41.59 | 14.5 | 2.2 | 0.5 | 5.5 | 3.34 | 32.37 |

### *2.2. Specimen Preparation*

In this study, five kinds of thermal insulation materials with different ratios were made by using the tailings of Guangxi Gaofeng Mine, P.O.32.5 cement, aluminum powder, VMB, quick lime, slaked lime, etc., and the ratios of each thermal insulation material are shown in Table 4.

**Table 4.** Mixing ratio of different thermal insulation materials.

| Number | Tailings/Part | VMB/% | Al/Part | Cement/Part |
|---|---|---|---|---|
| A | 65 | 5 | 1.5 | 18 |
| B | 55 | 15 | 1.5 | 14 |
| C | 55 | 10 | 1.0 | 10 |
| D | 65 | 15 | 1.0 | 14 |
| E | 65 | 5 | 0.5 | 10 |

According to the design of the test program and test methods for inorganic rigid thermal insulation (GB/T5486-2008) [19], the prepared specimens' mechanical properties included a test specimen size of 70.7 × 70.7 × 70.7 mm, with a thermal conductivity test specimen size of 300 × 300 × 30 mm in terms of thermal insulation. We conducted a determination of steady-state thermal resistance and related properties. Guarded hot-plate apparatus (GB/T10294—2008) was used [20]. Figure 1 is the flowchart for specimen production and specimen production steps are as follows:

1. Pre-treatment of raw materials: To avoid the long-term storage of tailings into blocks, the crusher or stone hammer is used for crushing, with dehydration and drying treatment at 105 °C to obtain dried fine particles of tailings.
2. Preparation of slurry: Weigh tailings, VMB, cement, quick lime, slaked lime, and other raw materials according to the proportion, put into the mixer, and dry mix for two minutes; according to the ratio of water to material, add a fixed amount of water, and pre-mix the mixer for two minutes. Finally, add aluminum powder and mix at a fixed speed for two minute; then, pour into the mold immediately.
3. Specimen preparation: The cleaned mold interior is coated with lubricant to facilitate the later demolding and then evenly loaded into the slurry after the initial maintenance at room temperature for 2 days.
4. Maintenance of specimen/conservation of specimens: After the completion of the initial maintenance of the specimen demolding, after the demolding of the mold into the constant-temperature and humidity box for maintenance, the maintenance temperature is set to 20 ± 2 °C, and the humidity is 98%.

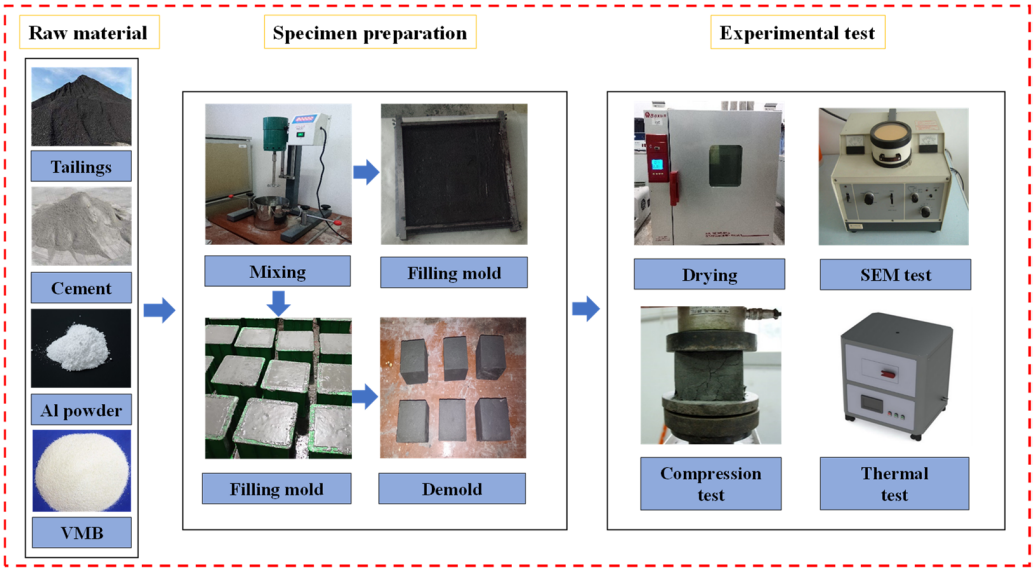


**Figure 1.** Experimental procedure.

## 3. Analysis of Results

### *3.1. Thermodynamic Properties and Microstructure of Thermal Insulation Materials*

#### 3.1.1. Microstructure of Thermal Insulation Material

Scanning electron microscopy (SEM) can fully characterize the pores, cracks, and microstructures within the material, allowing for a comprehensive observation of its internal structure. Therefore, SEM was used to observe the microstructure at each group level, with the results shown in Figure 2. The pores are irregular and unevenly distributed, with noticeable differences in porosity. The porosity of materials A-E was 9.7%, 10.3%, 12.1%, 17.0%, and 17.7%, respectively. Figure 2 indicates that in ratios A and B, with 1.5 parts of aluminum powder, the proportion of connecting holes is predominant. In ratios C and D, with 1 part of aluminum powder, the proportion of closed holes is higher. In ratio E, with 0.5 parts of aluminum powder, the number of both connecting and closed holes is smaller. During the mixing process, aluminum powder reacts with slaked lime to produce hydrogen, creating a gas–liquid interface between hydrogen and the slurry, which is an unstable thermodynamic structure. Thus, the slurry consistency directly affects the pore morphology of the material. The irregular and uneven distribution of pores suggests that the consistency of the sample-making slurry was low, causing hydrogen pores to rupture during the liquid discharge process. Consequently, the porosity was higher in ratios with a higher dosage of aluminum powder. Additionally, as the tailings content increases, the soil skeleton changes from agglomerated to primarily agglomerated, and the tailings themselves have low bonding strength, requiring more clinker to achieve a good bonding effect. The grain size of the tailings sand used in the experiment is small, necessitating a high water-to-material ratio, which decreases the consistency. The addition of a foam stabilizer and quick-setting agent is considered at a later stage to regulate the pore structure.

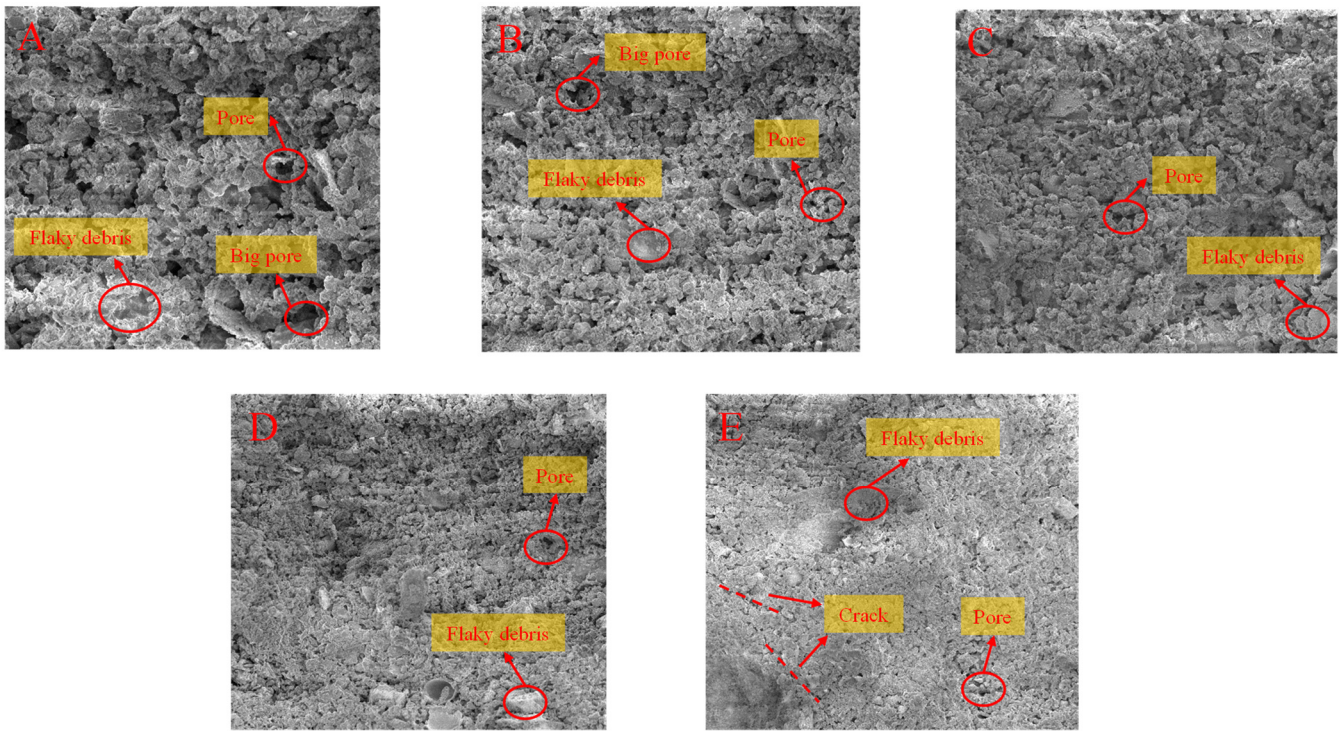


**Figure 2.** SEM observations results (**A**–**E**).

#### 3.1.2. Mechanical Properties of Thermal Insulation Materials

The experimental compressive strength data were obtained using a TYE-2000 pressure testing machine (made in China Wuxi Jianyi Instrument & Machinery Co., Ltd., Wuxi, China), and the compressive strength of each specimen was the arithmetic average of three randomly selected specimens, which was accurate to 0.01 MPa. Compressive strength

curves under five different ratios were obtained. The results of mechanical property tests are shown in Figure 3. The rupture condition of specimens with different test ratios varies, and the porosity of tailings-based thermal insulation material shows a quadratic function relationship with its compressive strength, with the function line opening downward.

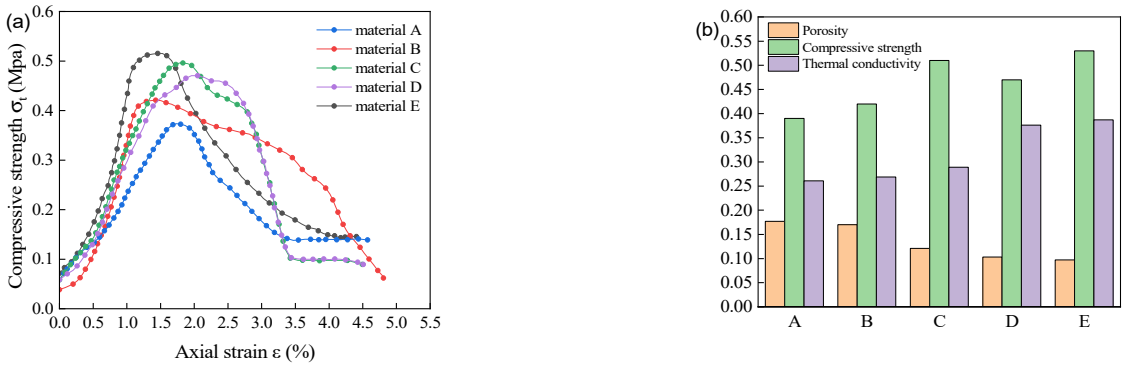


**Figure 3.** (**a**) Measurement curve of compressive strength of thermal insulation materials. (**b**) Measurement results of thermodynamic properties.

Usually, porosity is inversely related to compressive strength [21], and the critical strain of a porous matrix before reaching adequate strength is quantitatively associated with porosity. As seen from Table 5, there is no clear proportionality between the porosity and compressive strength of the five materials. This lack of proportionality can be attributed to two main reasons. First, the raw material tailings have low strength. When the amount of clinker is insufficient to bond the tailings particles, the system's compressive strength is low. Conversely, when the amount of cement clinker is adequate, but the amount of blowing agent is too high, the system becomes non-uniform under pressure, leading to numerous ruptures of the air holes, and the system still exhibits low compressive strength. When the dosage of aluminum powder is appropriate, the compressive strength of the system rises with the increase in clinker dosage; when the dosage of cement is relevant, but the dosage of the blowing agent is too high, the compressive strength of the system decreases.

**Table 5.** Measurement results of thermodynamic properties.

| Number | Tailings/Part | VMB/% | Al/Part | Cement/Part | Porosity/% | Compressive Strength (MPa) | Thermal Conductivity (W/(K·m)) |
|---|---|---|---|---|---|---|---|
| A | 65 | 5 | 1.5 | 18 | 17.7 | 0.39 | 0.261 |
| B | 55 | 15 | 1.5 | 14 | 17.0 | 0.42 | 0.269 |
| C | 55 | 10 | 1.0 | 10 | 12.1 | 0.51 | 0.289 |
| D | 65 | 15 | 1.0 | 14 | 10.3 | 0.47 | 0.376 |
| E | 65 | 5 | 0.5 | 10 | 9.7 | 0.53 | 0.387 |

### 3.1.3. Thermal Conductivity of Thermal Insulation Material

The steady-state method was chosen for thermal conductivity testing. Two specimens were randomly selected for each formulation, ensuring a thickness difference of no more than 2% between them, and both covered the surface of the heating unit. The surface of each specimen was ground flat with sandpaper to ensure close contact with the hot and cold plates, and the specimens were wrapped with plastic film on all sides. After determining the mass of each specimen, they were placed in an oven until they reached a constant weight. The temperature difference between the hot and cold plates was set to 10 °C, as read by the PDR 300 thermal conductivity dashboard. The arithmetic average of the measurements was taken as the thermal conductivity value for each group, with the data shown in Table 5.

The tailings-based thermal insulation materials belong to the inorganic thermal insulation mortar category, and their thermal conductivity was determined directly from the thermal conductivity instrument panel. The measured thermal conductivity of five different thermal insulation materials was 0.261, 0.269, 0.289, 0.376, 0.387 W/(K·m), with a maximum of 0.387 W/(K·m) and a minimum of 0.261 W/(K·m), all showing good thermal insulation performance. As shown in Figure 3, the thermal conductivity shows a decreasing trend with increasing porosity. In contrast, the porosity of A–E depends on the content of aluminum powder and Vitrified Micro Bubbles in the ratios and with the increase in aluminum powder. Dense and tiny pores begin to form inside the material, and the thermal conductivity of the air inside the pores is much smaller than the solid thermal conductivity, so the thermal conductivity decreases significantly. Its dosage will also increase its porosity, thus reducing the thermal conductivity. Still, from the experimental results in Table 5, when the amount of aluminum powder is the same, the amount of VMB in ratios B and D is more significant than that of A and C. However, its porosity is even lower, which may be because of the long mechanical mixing process, in which the VMB, which has a porous structure, will become less porous. The reason for this may be that during the extended mechanical mixing process, the original porous structure of the glass beads becomes smaller particles. These particles will be filled into the voids, so that the porosity of the material in the mixing does not increase but, rather, decreases.

### *3.2. Analysis of the Cooling Performance of Surrounding-Rock Thermal Insulation Materials*

After preparing the thermal insulation material for surrounding rock, due to the need to apply and mine production blindly and directly in the field test, there are many extreme conditions, such as the high-temperature environment of the deep mine, complex geological conditions, long time verification, etc. Numerical simulation can address these challenges by providing reliable data support and a theoretical basis for practical application. Additionally, numerical simulation can also save the consumption of human, material, financial, and other resources for on-site testing. The test results are now simulated and analyzed under different thermal-insulation-layer thicknesses, thermal conductivity, inlet wind speed, and raw rock temperatures for the cooling effect of thermal insulation material, and the results obtained are as follows.

#### 3.2.1. Roadway Surrounding-Rock Model and Parameter Setting

The model roadway is a three-center arch; the width of the roadway is 4 m, and the height of the wall is 4 m; the radius of the surrounding rock of the roadway is set to 20 m; and the length of the roadway is set to 300 m. ANSYS(2022 R1) SpaceClaim module (ANSYS, Inc., Canonsburg, PA, USA) was used for the modeling and analysis, and the constructed three-dimensional model was imported into Fluent for the mesh delineation and computational solution. The number of meshes is approximately 160,576,762. Here, the thermal conductivity of the prepared material is selected, and the thickness of the mine thermal insulation layer is generally 5–25 cm and compared with the uncoated case to study whether the prepared thermal insulation and cooling material is effective for the cooling of the roadway; the outer surface temperature of the surrounding rock is set to be 40 °C, the inlet wind speed is set to be 1 m/s, the temperature is 24 °C, and the thermal conductivity of the surrounding rock is 2.5 W/(K·m).

#### 3.2.2. Influence of the Thickness of the Insulation Layer on the Temperature of the Wind Flow in the Roadway

The thickness of the roadway thermal insulation layer significantly affects the roadway temperature. Thermal insulation material A, with a thermal conductivity of 0.261 W/(K·m), was selected as the spray material. The thickness of the thermal insulation layer was set to 0, 5, 10, 15, 20, and 25 cm. The change in roadway wind flow under different thermal insulation layer thicknesses was obtained through simulation. As shown in Figure 4a, the

horizontal coordinate 0 indicates the beginning of the roadway, and 300 m indicates the exit of the roadway.

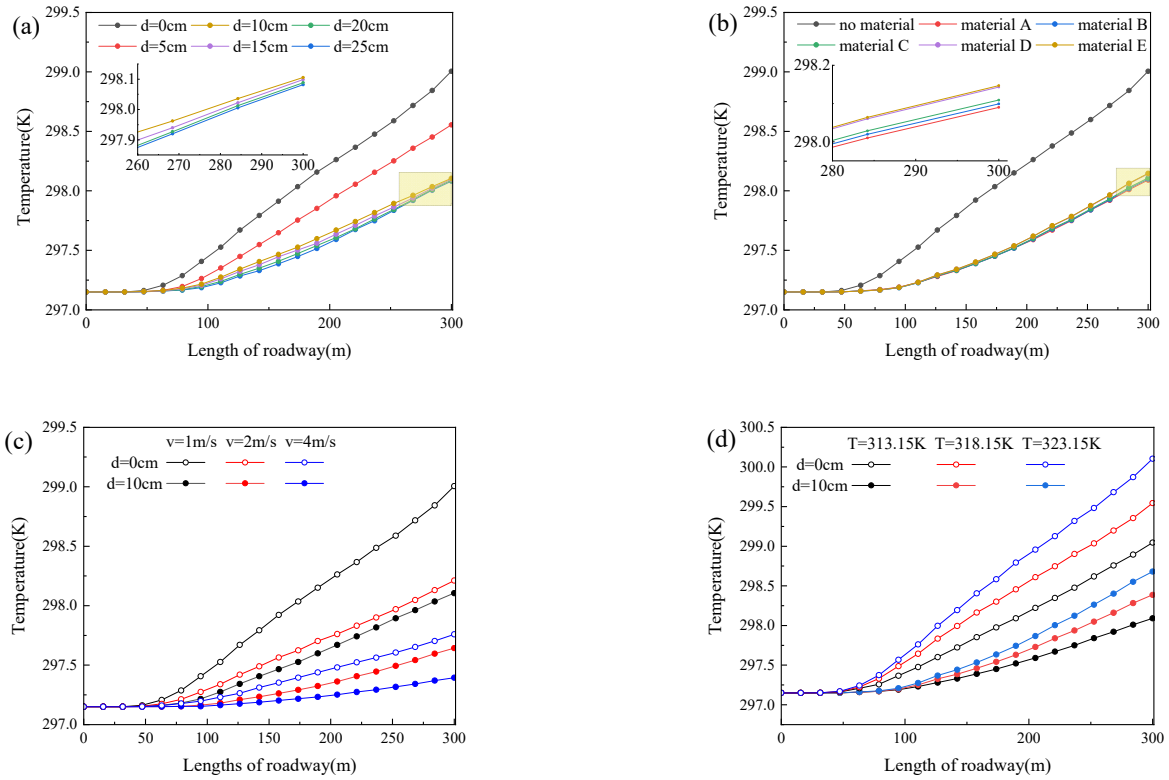


**Figure 4.** (**a**) Temperature variation of airflow in the center of the roadway with different insulation thicknesses. (**b**) Temperature variation of airflow in the center of the roadway with different thermal conductivities. (**c**) Temperature variations of the wind flow in the center of the roadway at different inlet wind speeds. (**d**) Temperature variations of airflow in the center of the roadway at different surrounding rock temperatures.

Figure 5 is a cloud diagram of the temperature distribution showing the roadway sprayed with different thicknesses of heat-insulating coatings. As can be seen from the temperature change rules of the outer wall surface of the roadway shown in Figure 5a–f, the temperature of the roadway with the sprayed thermal insulation coating is lower, which can effectively reduce the heat transfer from the surrounding rock to the airflow in the roadway. In particular, compared to the unsprayed roadway (Figure 5a), the rate of increase in the airflow temperature in the sprayed roadway (Figure 5f) with a 25 cm thermal insulation coating thickness was significantly reduced. Figure 6a shows a temperature distribution cloud of the exit surface of the roadway. With the thermal insulation coating, there is a significant decrease in temperature compared to the roadway without a thermal insulation coating. When air passes through the roadway with thermal insulation coating, the outer coating acts as a heat insulator for the air temperature within the roadway. It inhibits the roadway from directly absorbing the heat from the surrounding rock.

From Figure 4a, it can be seen that the temperatures of the wind flow at the center of the roadway exit are 299.01 K, 298.55 K, 298.11 K, 298.10 K, 298.09 K, and 298.08 K. The roadway temperature is significantly reduced after adding the heat insulation layer. The maximum decrease in the wind flow temperature at the center of the roadway exit is 0.93 K. When the thickness of the thermal insulation layer is increased from 5 cm to 10 cm, the roadway temperature decreases by 0.45 K. However, when it is increased from 10 cm to 25 cm, the temperature of the roadway decreases by only 0.03 K. Considering the cost and other related factors, the comprehensive benefit of choosing the thermal insulation material with a thickness of 10 cm is clear.

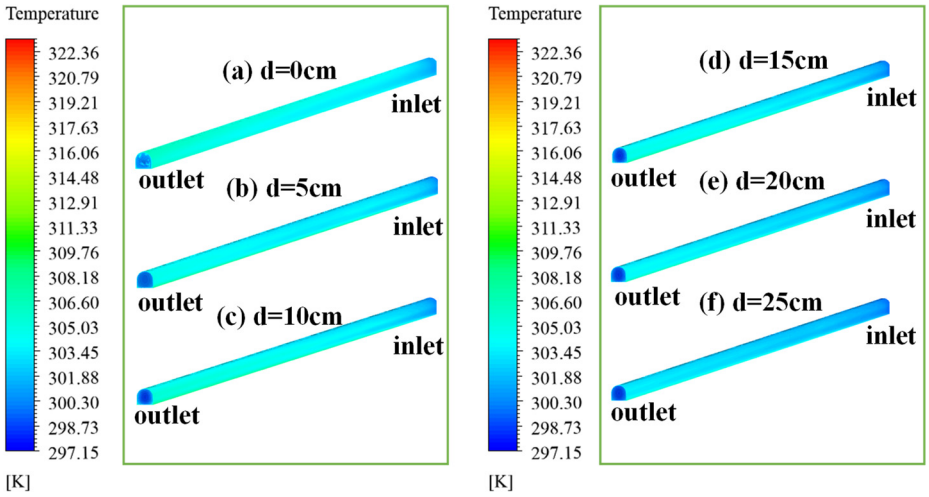


**Figure 5.** Distribution of roadway temperatures with different insulation coating thicknesses.

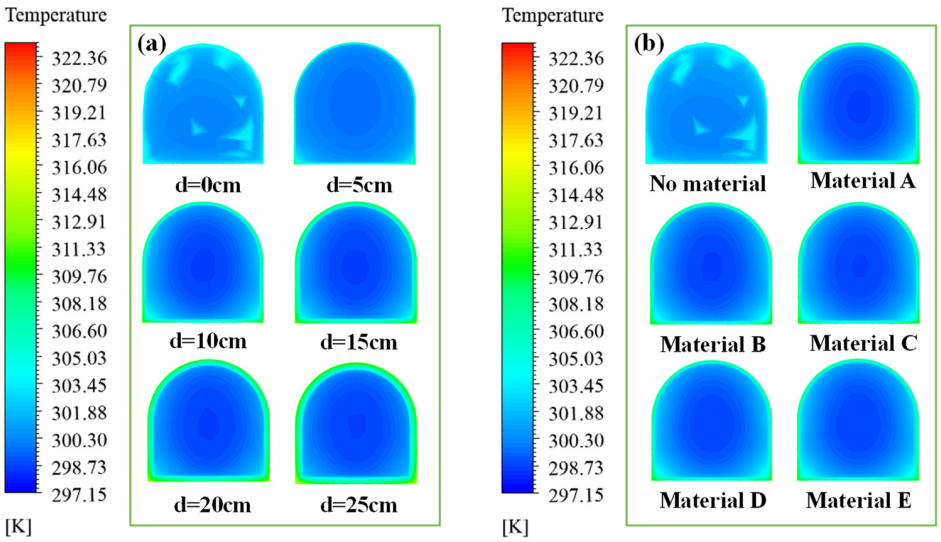


**Figure 6.** (**a**) Distribution of roadway exit temperatures with different insulation coating thicknesses. (**b**) Distribution of roadway exit temperatures to varying degrees of thermal conductivity.

### 3.2.3. Influence of Thermal Conductivity of Thermal Insulation Materials on the Temperature of the Airflow in the Roadway

The thermal conductivity of the five thermal insulation materials prepared was selected to study the effect of different insulation material thermal conductivities on the temperature of the wind flow in the mine roadway at a coating thickness of 10 cm.

Figure 6b shows a temperature distribution cloud diagram of the exit surface of the roadway under spraying thermal insulation materials with different thermal conductivities, according to the color of the exit surface spraying thermal insulation material and the other five groups. It is evident that the temperature is significantly reduced in the roadway with a thermal insulation coating compared to the one without it. The low-temperature region increases at the center of the roadway from material A to material E. When air passes through a roadway with thermal insulation material, the different thermal conductivities of the coatings have varying degrees of influence on the cooling effect of the roadway.

From Figure 4b, it can be seen that the temperatures of the wind flow at the center of the roadway exit are 299.01 K, 298.15 K, 298.14 K, 298.11 K, 298.10 K, and 298.09 K. After adding the thermal insulation layer, the rate of temperature increase in the wind flow in the roadway gradually became smooth. The temperature of the wind flow in the center of the roadway exit was reduced by up to 0.92 K, and the temperature change was reduced by

47.22%. Comparing the five different materials, it was found that the temperature of the thermal insulation material with higher thermal conductivity was generally higher than that of the material with lower thermal conductivity. This means that the lower the thermal conductivity of the thermal insulation material, the lower the temperature of the wind flow at the exit of the roadway, resulting in a better thermal insulation effect.

#### 3.2.4. Influence of Inlet Wind Speed on the Temperature of the Wind Flow in the Roadway

Mines in the same region have different geothermal gradients. For some mining roadways with more thermal severe damage, it is difficult to achieve an excellent cooling effect on the working environment simply by adding surrounding-rock thermal insulation material. Therefore, the problem of high-temperature environments on work surfaces can be solved by combining insulating coatings with ventilation measures. In the case of inlet wind speeds of 1 m/s, 2 m/s, and 4 m/s, we conducted a simulation study on the influence of the presence or absence of a heat insulation layer on the temperature of the roadway to obtain the distribution of the ventilation temperature of the roadway under different inlet wind speeds. The temperature distribution of the roadway ventilation at different inlet wind speeds is obtained. Figure 7a shows a cloud view of the temperature distribution at the exit face of the roadway for varying inlet wind speeds. There is a significant reduction in temperature when there is a thermal insulation coating compared to the roadway without thermal insulation coating.

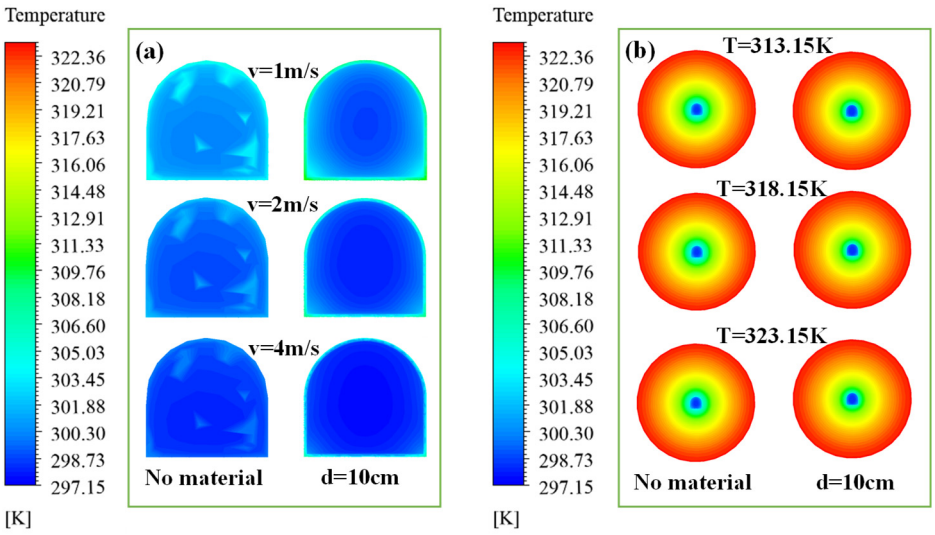


**Figure 7.** (**a**) Distribution of roadway exit temperatures at different inlet wind speeds. (**b**) Temperature distribution of the surrounding rock at different surrounding-rock temperatures.

From Figure 4c, it can be seen that the temperature difference between the wind flow in the center of the roadway with and without the heat insulation layer increases significantly as the inlet wind speed decreases. When the inlet wind speed is 4 m/s, the temperature difference at the roadway exit section is 0.37 K; when the inlet wind speed is 2 m/s, the temperature difference of the roadway exit section is 0.57 K; when the inlet wind speed is 1 m/s, the temperature difference of the roadway exit section is 0.9 K. For the same inlet wind speed, the temperature difference between the roadway with insulation and the roadway without insulation increases as the length of the roadway increases. Therefore, when the inlet wind speed of the roadway is lower and the roadway is longer, the cooling effect of the thermal insulation material is more prominent.

#### 3.2.5. Influence of Surrounding-Rock Temperature on Roadway Temperature

The raw rock temperature has a significant effect on both the roadway temperature and the surrounding-rock thermoregulation circle. Surrounding-rock temperatures of 40 °C,

45 °C, and 50 °C at the outer wall were selected to explore the effects of spraying the thermal insulation layer on the roadway temperature and the surrounding-rock thermoregulation circle under different surrounding-rock temperatures.

Figure 4d shows a temperature variation curve along the center of the roadway when the surrounding-rock temperature is different. It can be seen that with an increase in the surrounding-rock temperature, the temperature difference between the wind flow in the roadway with and without the heat insulation layer increases significantly, and the temperature difference between the roadway exit section is 0.92 K when the surrounding-rock temperature is 313.15 K; when the surrounding-rock temperature is 318.15 K, the temperature difference is 1.15 K; when the surrounding-rock temperature is 323.15 K, the temperature difference is 1.42 K. Additionally, for the same initial temperature of the surrounding rock, the temperature difference between the roadway with a thermal insulation layer and the roadway without it increases with the length of the roadway. Therefore, when the surrounding-rock temperature of the roadway is higher and the roadway is longer, the cooling effect of the thermal insulation material is more prominent.

Figure 7b shows a temperature-field variation cloud diagram in the surrounding-rock section. From Figure 7b, it can be seen that at three different surrounding-rock temperatures, the radius of the thermoregulation circle increases as the surrounding-rock temperature increases simultaneously. From Figure 7b, it can be seen that at three different surrounding-rock temperatures, the radius of the thermoregulation circle increases as the surrounding-rock temperature increases. Comparing the roadway with thermal insulation, it was found that the radius of the control heat circle appeared to be reduced after adding the thermal insulation layer at different temperatures. This is because the thermal conductivity of the insulation material is much lower than that of the surrounding rock, thus isolating the heat transfer between the surrounding rock and the roadway and reducing the radius of the control heat circle.

## 4. Conclusions

Tailings, P.O.32.5 cement, aluminum powder, vitrified micro bubbles, quick lime, and slaked lime were mixed in different ratios to produce five types of thermal insulation materials with different surrounding-rock thermodynamic properties and the cooling effect by simulating different working conditions. The conclusions are as follows:

1. Through the thermodynamic performance test, it was found that the overall performance of the five thermal insulation materials specimens was superior, with a thermal conductivity of 0.261–0.387 W/(K·m), which is an excellent thermal insulation performance. Still, their compressive strength of up to 0.53 MPa is unsuitable for use in a support structure for a roadway in a mine. After the roadway support structure is constructed, a heat-insulating coating can be added to the roadway surface to slow the heat transfer from the surrounding rock to the roadway.
2. By simulating and analyzing the influence of the thermal insulation layer on the temperature of wind flow in the roadway, we found that the thermal conductivity of thermal insulation materials and the thickness of the thermal insulation layer are the main factors affecting the cooling effect of roadway thermal insulation. The lower the thermal conductivity of the thermal insulation materials, the more significant the cooling effect; the greater the thickness of the thermal insulation layer, the better the cooling effect. The cooling effect of the thermal insulation layer is significantly reduced when the thickness of the thermal insulation layer exceeds 10 cm.
3. The cooling effect of the peripheral-rock thermal insulation coating was analyzed using Fluent numerical simulation software. For some mines with high-temperature thermal hazards, the addition of the thermal insulation layer and improvements in ventilation measures can be used to reduce the temperature of the roadway. Specifically, when the ambient rock temperature reaches 323.15 K and the ventilation conditions are poor, adding a 10 cm thick thermal insulation coating can effectively reduce the heat exchange between the surrounding rock and the roadway and reduce

the surrounding-rock heat-regulating circle to protect the operating personnel from high-temperature heat damage.

**Author Contributions:** Conceptualization, H.D. and Y.X.; methodology, Y.X.; validation, H.D.; investigation, Y.X.; writing—original draft preparation, Y.X.; writing—review and editing, H.D. and Y.X.; visualization, Y.X.; supervision, H.D. All authors have read and agreed to the published version of the manuscript.

**Funding:** This work was financially supported by the National Natural Science Foundation of China (funder: Hongwei Deng; Grant number: 51874352).

**Data Availability Statement:** All data in this study were obtained from our experiment and are authentic and reliable. The publication of data has the consent of all authors.

**Conflicts of Interest:** The authors declare no conflicts of interest.

## References

1. Ranjith, P.G.; Zhao, J. Opportunities and Challenges in Deep Mining: A Brief Review. *Engineering* **2017**, *3*, 546–551. [CrossRef]
2. You, S.; Sun, J.C. Analysis of Thermal Environment and Its Influencing Factors in Deep Stope of Metal Mine. *Geofluids* **2022**, *2022*, 6408714. [CrossRef]
3. Roghanchi, P.; Kocsis, K.C. Challenges in Selecting an Appropriate Heat Stress Index to Protect Workers in Hot and Humid Underground Mines. *Saf. Health Work-Kr.* **2018**, *9*, 10–16. [CrossRef] [PubMed]
4. Han, Q.Y.; Zhang, Y. Computational evaluation of cooling system under deep hot and humid coal mine in China: A thermal comfort study. *Tunn. Undergr. Space Technol.* **2019**, *90*, 394–403.
5. Nie, X.X.; Wei, X.B. Heat Treatment and Ventilation Optimization in a Deep Mine. *Adv. Civ. Eng.* **2018**, *2018*, 1529490. [CrossRef]
6. Miao, D.J.; Sui, X.H. Adequate air volume in working face after mechanical refrigeration. *Saf. Sci.* **2012**, *50*, 705–708. [CrossRef]
7. Zhang, X.; Zhang, S. Performance Test and Thermal Insulation Effect Analysis of Basalt-Fiber Concrete. *Materials* **2022**, *15*, 8236. [CrossRef] [PubMed]
8. Zhang, S.; Xue, X. Current situation and comprehensive utilization of iron ore tailing resources. *J. Min. Sci.* **2006**, *42*, 403–408. [CrossRef]
9. Chen, L.H.; Li, Q. Comprehensive Utilization of Tailings in Quartz Vein-Hosted Gold Deposits. *Minerals* **2022**, *12*, 1481. [CrossRef]
10. Jin, C.; Liu, H. Experimental study on tailings cementation by MICP technique with immersion curing. *PLoS ONE* **2022**, *17*, e0272281. [CrossRef] [PubMed]
11. Huiskes, D.; Keulen, A. Design and performance evaluation of ultra-lightweight geopolymer concrete. *Mater. Des.* **2016**, *89*, 516–526. [CrossRef]
12. Demirboga, R.; Gül, R. The effects of expanded perlite aggregate, silica fume and fly ash on the thermal conductivity of lightweight concrete. *Cem. Concr. Res.* **2003**, *33*, 723–727. [CrossRef]
13. Soltan, A.; Pöhler, K. Clay-bricks from recycled rock tailings. *Ceram. Int.* **2016**, *42*, 16685–16696. [CrossRef]
14. Qin, Q.Z.; Geng, H.H. Al and other critical metals co-extraction from coal gangue through delamination pretreatment and recycling strategies. *Chem. Eng. J.* **2023**, *477*, 147036. [CrossRef]
15. Rao, P.S.; Chandar, K.R. Development of energy efficient organic bricks in construction using IOT and perlite. *Int. J. Sustain. Eng.* **2021**, *14*, 865–873.
16. Hu, S.T.; Xiong, X.H. Characterization and utilization potential of typical molybdenum tailings in Shaanxi Province, China. *Environ. Geochem. Health* **2024**, *46*, 265. [CrossRef] [PubMed]
17. Yao, W.; Lyimo, H. Evolution regularity of temperature field of active heat insulation roadway considering thermal insulation spraying and grouting: A case study of Zhujidong Coal Mine, China. *High Temp. Mater. Process.* **2021**, *40*, 151–170. [CrossRef]
18. Hou, C.; Xin, S. Foundation Research on Physicochemical Properties of Mine Insulation Materials. *Coatings* **2020**, *10*, 355. [CrossRef]
19. Xu, W.; Tian, X. Experimental study on the pore and strength properties of cemented unclassified during the consolidation process. *J. China Univ. Min. Technol.* **2016**, *45*, 272–279.
20. *GB/T 5486-2008*; Test Methods for Inorganic Rigid Thermal Insulation. Standards Press of China: Beijing, China, 2008. (In Chinese)
21. *GB/T 10294-2008*; Thermal Insulation. Determination of Steady-State Thermal Resistance and Related Properties. Guarded Hot Plate Apparatus. National Quality Supervision Bureau: Beijing, China, 2008. (In Chinese)